Vol. 18, No. 2 (2019) 737-747
Revista Mexicana de Ingeniería Química

INCORPORATION OF CIPROFLOXACIN/BETA CYCLODEXTRIN INCLUSION COMPLEX TO POLYLACTIC ACID ELECTROSPUN FIBERS AND MODELING OF THE RELEASE BEHAVIOR

INCORPORACIÓN DEL COMPLEJO DE EXCUSIÓN DE CIPROFLOXACINO/BETA CICLODEXTRINA A FIBRAS ELECTROHILADAS DE ÁCIDO POLILÁCTICO Y EL MODELAMIENTO DEL COMPORTAMIENTO DE LIBERACIÓN

G.M. Estrada-Villegas[1,2], R.C. Martínez- Hernández[1], J. Morales[1], R. Olayo[1]*

[1] *Departamento de Física, Universidad Autónoma Metropolitana Iztapalapa, Avenida San Rafael Atlixco 186, Colonia Vicentina, 09340 Iztapalapa, CDMX, México.*
[2] *CONACyT-Centro de Investigación en Química Aplicada, Av. Alianza Sur 204 Parque de Innovación e Investigación Tecnológica, Apodaca, Nuevo León, 66629 México.*

Received: January 1, 2019; Accepted: March 19, 2019

Abstract

The ciprofloxacin (CIP) hydrophobic drug and its inclusion complex, β-cyclodextrin-CIP (IC) were encapsulated into micro- and nano-fibers of polylactic acid (PLA) via electrospinning technique to evaluate CIP release mechanism. The IC was characterized by 13C solid-state nuclear magnetic resonance (SSNMR) and thermogravimetric analysis (TGA) to investigate the inclusion of complex formation. The PLA-IC and PLA-CIP fibers were characterized by TGA, Raman spectroscopy and scanning electron microscopy (SEM). The release behavior of CIP as well as the loading efficiency percentage (LE%) was evaluated via UV-Vis at 276 nm. Results showing that IC inclusion complex improves the loading efficiency and also increase the control in drug release rate when compared with only CIP. That means CIP was released in a more prolonged and sustained manner from PLA-IC fibers versus PLA-CIP fibers. Different PLA-CIP and PLA-IC fiber diameters did not influence the release profile of the drug. The experimental results of CIP releasing were approximated with three commonly used semi-empirical models: Korsmeyer-Peppas, zero-order, and first-order kinetic equation to explain the release mechanism. The Korsmeyer-Peppas model showed the best fit to the PLA-CIP while the first-order model describes the best fit to PLA-IC as a consequence of the delayed release of CIP in IC.

Keywords: cyclodextrin, electrospinning, inclusion complex, fiber, kinetics model.

Resumen

El fármaco hidrofóbico de ciprofloxacina (CIP) y su complejo de inclusión, β-ciclodextrina-CIP (IC) se encapsularon en microfibras y nanofibras de ácido poliláctico (PLA) mediante técnica de electrohilado para evaluar el mecanismo de liberación de CIP. El IC se caracterizó por resonancia magnética nuclear de estado sólido 13C (SSNMR) y análisis termogravimétrico (TGA) para investigar la formación de complejo de inclusión. Las fibras PLA-IC y PLA-CIP se caracterizaron por TGA, espectroscopia Raman y microscopía electrónica de barrido (SEM). El comportamiento de liberación de CIP, así como el porcentaje de eficiencia de carga (LE%) se evaluaron mediante UV-Vis a 276 nm. Los resultados muestran que el complejo de inclusión de IC mejora la eficiencia de carga y también aumenta el control en la tasa de liberación del fármaco cuando se compara con solo el CIP. Eso significa que el CIP se liberó de una manera más prolongada y sostenida de las fibras de PLA-IC en comparación con las fibras de PLA-CIP. Diferentes diámetros de fibra PLA-CIP y PLA-IC no influenciaron el perfil de liberación del fármaco. Los resultados experimentales de la liberación de CIP se aproximaron con tres modelos semi-empíricos de uso común: Korsmeyer-Peppas, orden cero y ecuación cinética de primer orden para explicar el mecanismo de liberación. El modelo de Korsmeyer-Peppas mostró el mejor ajuste para el PLA-CIP, mientras que el modelo de primer orden describe el mejor ajuste para el PLA-IC como consecuencia de la liberación retardada del CIP en el IC.

Palabras clave: ciclodextrina, electrohilado, complejo de inclusión, fibra, modelo cinético.

* *Corresponding author. E-mail*: oagr@xanum.uam.mx
https://doi.org/10.24275/uam/izt/dcbi/revmexingquim/2019v18n2/Estrada
issn-e: 2395-8472

1 Introduction

The goal of nanofiber tissue engineering scaffold design is to provide an ideal structure that can replace the natural extracellular matrix until the host cells can grow and synthesize a new natural cellular matrix (Wendorff, *et al*. 2012; Salgado-Delgado, *et al*. 2016) Extensive studies have been conducted to develop biocompatible fibrous mats as scaffolds including the biodegradable polymer polylactic acid (PLA) that is a biodegradable aliphatic polyester (Auras *et al*., 2004).

Electrospinning is a common and versatile technique for producing nano- and micro-fibers from polymer solutions via a very strong electric field (Greiner and Wendorf,f, 2007; Ledezma-Oblea, *et al*. 2015). Electrospun fiber membranes containing antibiotic agents have been used as a barrier to prevent post-wound infections. Of these, the fluoroquinolone antibiotic ciprofloxacin (CIP) is one of the most common antibiotics to treat different bacterial infections including anthrax, bones and joints, endocarditis, gastroenteritis, malignant otitis externa, respiratory tract infections, urinary tract infections, prostatitis, and chancroid. CIP is a widely used antibiotic with a low minimal inhibitory concentration for both Gram-positive and Gram-negative bacteria; the frequency of spontaneous resistance to ciprofloxacin is very low (Rajendiran, *et al*., 2016; Bukovec and Quirds, 1997).

Cyclodextrins (CDs) are natural cyclic oligosaccharides with a cavity size varying from 0.5-1 nm. (Szejtli, 1994). CDs can form non-covalently bonded inclusion compounds with small molecules and polymers via inclusion of these guest molecules in their small cavities. They form inclusion complexes with several drugs because of their special molecular structure, hydrophobic internal cavity, and hydrophilic external surface. Be able to also reduce toxicity and control the rate of release, can improve solubility, lower toxicity, and increase bioavailability of these drugs (Jannesari, *et al*., 2011).

Recently, the first reports of the incorporation of fluoroquinone antibiotics by electrospinning in fibrous materials have been appeared with poly (vinyl alcohol) (PVA) and PVA/poly(vinyl acetate) (Shawki, *et al*., 2010), dextran (Choia, *et al*., 2013), poly urethane (PU) (Toncheva, *et al*., 2012), poly(D,L lactide acid) (PDLLA)/poly(ethylene oxide) (PEO) (Bottino, *et al*., 2014), polydioxane (PDN) (Ahire, *et al*., 2015), and poly(D,L lactide acid) (PDLLA)(Buvári, *et al*., 1998). Nevertheless, the effect of β-CD-/IC on release behavior of CIP from polymer micro- and nano-fibers has not yet been investigated.

Studies have shown that other inclusion complexes can be encapsulated in polymers fibers. This leads to a higher loading efficiency and control release when compared with no encapsulated molecules (Aytac, *et al*., 2015). CIP was chosen as the reference drug because of its well-known inclusion complex formation ability with beta-cyclodextrin (β-CD) (Jianbin, *et al*., 2012). Several characterization tests were performed to confirm the formation of the inclusion complex. The release profiles of CIP and IC after incorporation into PLA fibers (PLA/CIP and PLA/IC) by electrospinning were examined in PBS 7.4 buffer solutions by UV-Vis absorption at 276 nm. The main objective of this study was to enhance the release profile of CIP from PLA/IC fibers, increase the CIP loading efficiency and control release, when compared with only PLA-CIP. Semi-empirical models: Korsmeyer-Peppas, zero-order, and first-order kinetic were used to explain the influence of IC incorporation on micro and nanofibers and try to predict the release behavior to extent to another system.

2 Materials

The Mw 45000 IngeoTM Biopolymer PLA from Nature Worrks LLC-USA was used to obtain polymer micro and nanofibers. Ciprofloxacin from Novak-Euflexin from Euromex-México laboratories was previously purified by crystallization. Dichloromethane (DCM), chloroform, and dimethyl sulfoxide (DMSO) were from Sigma Aldrich - USA and used as received. The β-CD was from Sigma Aldrich-USA. PBS from Aldrich was used as a received. The water was distilled water deionized from a Millipore Milli-Q ultrapure water system.

3 Experimental

3.1 *Preparation of solid complex of CIP with β-CD*

The preparation of the solid IC used a co-precipitation method: 0.567 g of β-CD (0.5 mmol) was dissolved in 30 mL of distilled water. Next, 0.199 g of CIP (0.6

mmol) was dissolved in 20 mL of distilled water and stirred until complete dissolution. The β-CD solution was then poured dropwise into the ciprofloxacin solution and continually stirred for 12 h at 45 °C. The reaction mixture was kept at 4 °C for 24 h. Then precipitated crystals were filtered and washed with distilled water and triturated in an agate mortar and then dried in an oven at 60 °C for 24 h. A white powdered product was obtained.

3.2 Preparation of electrospinning solutions

The CIP and IC were incorporated into PLA fibers via electrospinning. Here, free CIP (5%, w/w, with respect to polymer) was dissolved in 10 mL of DCM: DMSO (8:2) at room temperature (RT). Then, 1 g of PLA was added to the mixture; PLA/CIP solution was stirred for 120 min before electrospinning. To make PLA/IC fibers, IC (5% CIP, w/w, with respect to polymer) was dispersed in 10 mL of DCM: DMSO (8:2) at RT. Afterward, 1g of PLA was added, and the PLA/IC solution was stirred for 120 min prior to electrospinning. In the case of CIP, the drug was dissolved as good as possible, but a milky white suspension was obtained. The control solution was 1 g of PLA in 10 mL of DCM: DMSO (8:2).

3.3 Electrospinning of PLA/CIP, PLA, and PLA/IC solutions

Electrospinning was done in a TL-01 (TONGLI) machine. The PLA/CIP suspension, PLA, and PLA/IC solutions were individually loaded into a 20 mL plastic syringe with a 22-gauge needle placed on the syringe pump. The flow rate of the polymer solutions was 1 mL/h. The metal plate collector was 15 cm from the needle tip and covered with aluminum foil. The ground and the positive electrodes of the high voltage power supply were clamped to the collector and the needle, respectively. The electrospinning was performed at 18 kV and 30 °C. This process is shown in Figure 1.

3.4 Characterization

The formation of IC was confirmed by solid proton nuclear magnetic resonance (13C NMR, Bruker D PX-400) system and thermogravimetric analysis (Pyris 1, Perkin Elmer). The spectra were recorded at 400 MHz over 16 total scans. The scanning electron microscope (SEM) (JEOL JSM 7600F scanning microscope) was

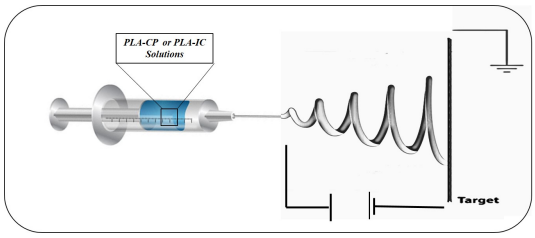

Fig. 1. Simplified scheme of PLA CIP or IC electrospinning process.

used for the morphological analysis of the electrospun micro and nanofibers. Samples were sputtered with 5 nm Au prior to SEM imaging. The average fiber diameter (AFD) was determined from the SEM images, and around 25 fibers were analyzed. The thermal properties of the electrospun fibers were studied by TGA, and the measurements were carried out performed from 25 to 600°C at a 10 °C min^{-1} heating rate; N_2 was used as the purge gas. The Raman spectra of the fibers were obtained with a WITEC, ALPHA300 RA + microscope. The 32 replicate scans were recorded between 3700 cm^{-1} and 200 cm^{-1} at a resolution of 4 cm^{-1}.

3.5 The CIP release profile from electrospun PLA fibers

The amount of CIP cumulatively released from the PLA/CIP fibers and the PLA/IC fibers was studied in vitro at 37 °C in a phosphate buffer (NaH_2PO_4/KH_2PO_4) at pH 7.4 0.5 $molL^{-1}$ and an ionic strength of 0.1. Fibers (6 mg) were immersed in 10 mL of aqueous buffer solution and continuously stirred at 150 rpm. The release kinetics were measured by periodically withdrawing 0.5 mL aliquots and adding an equal volume of fresh medium. The absorbance of these solutions was recorded at 276 nm. The amount of antibiotic released over time was calculated using calibration curves (correlation coefficient R~ 0.99) in phosphate buffer.

The experiments were performed by triplicate. The loading efficiency (LE) (%) of PLA/CIP fibers and PLA/CIP/βCD-IC fibers were determined by dissolving 5 mg of nanofiber in 5 mL of DCM; the amount of CIP in the nanofiber was determined by a UV-Vis curve. Finally, the LE% was calculated according to the following equation (Eq. 1):

$$LE(\%) = \frac{Ce}{CtX100} \quad (1)$$

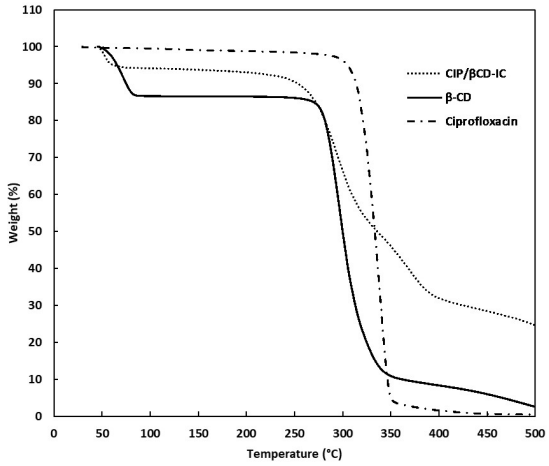

Fig. 2. Thermal degradation behavior of Inclusion complex.

where Ce is the concentration of encapsulated active compound, and Ct is the total concentration of the active compound.

4 Results and discussion

4.1 Inclusion complex characterization

The IC was further investigated by TGA to determine the thermal stability and complex formation (Fig. 2). TGA of CIP and β-CD are also shown to the comparison. The thermal degradation of CIP had a one-step weight loss to main degradation at 280°C. The β-CD lost weight in two distinct steps: The first one corresponds to dehydration of the molecule, and the second one is the degradation of pyranose rings at 300°C. Thermal degradation behavior of IC exhibited a water loss about 5%, but this was only 17% for βCD. The 12% difference might be attributable to the existence of CIP instead of water in the βCD cavity. There is one weight loss step seen for IC around 290 °C this corresponds to free CIP and IC weight loss that merged with the CD decomposition. The relatively lower amount of uncomplexed free CIP suggests formation of the IC.

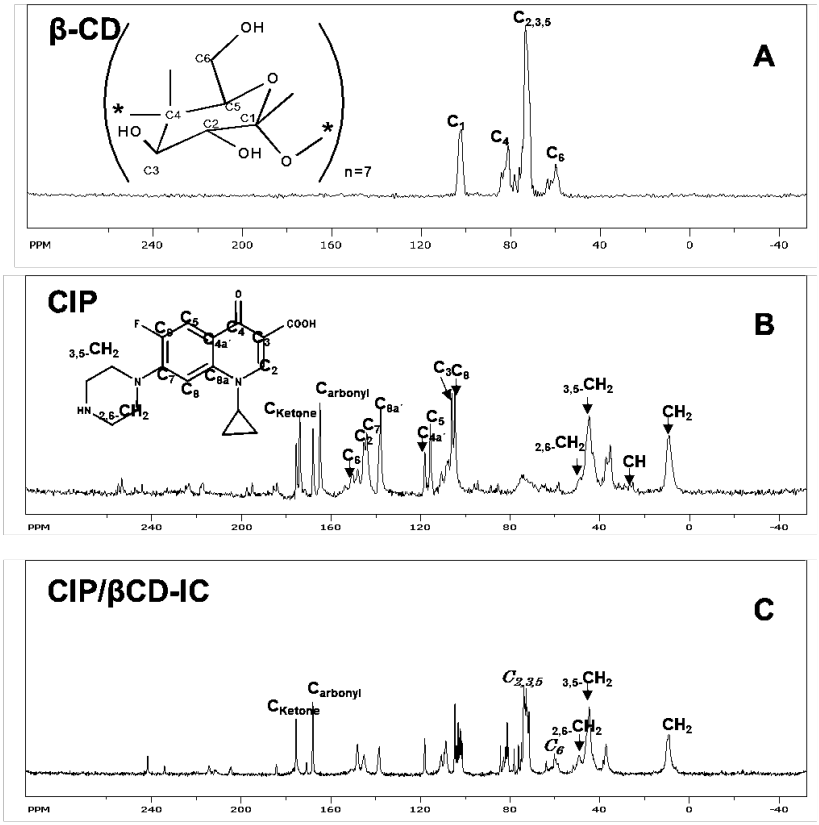

Fig. 3. RMN characterization of the CIP-βCD inclusion complex and its components.

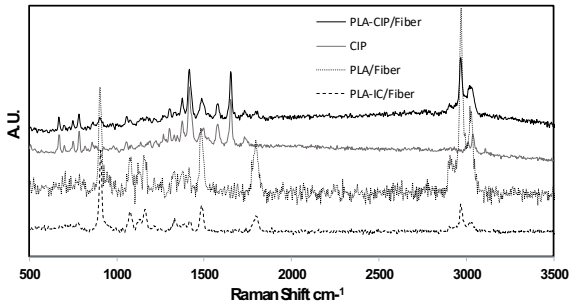

Fig. 4. Raman spectra of PLA fibers and loaded PLA fibers.

The IC was confirmed by analyzing the differences in the chemical shifts and modification of the peaks between the free and complexed molecules via 13C NMR. Figure 3A shows the βCD peaks from C1 to C6; its δC values are 104 (C1), 76.3 (C2, C3, C5), 84 (C4), 58.3 (C6). The appearance of multiple resonances for atoms C2, C3, C5, C4, and C6 of the glucopyranose units indicates the coexistence of different structural arrangements18. Figure 3B shows the characteristic 13C RMN for CIP: 9.5 (CH_2, cyclopropyl), 35.8 (CH, cyclopropyl), 45.3 (3/5-CH_2, piperazine), 50.7 (2/6-CH_2, piperazine), 106.0 (C-8), 107 (C-3), 115 (C-5), 118.3 (C-4a´), 138 (C-8a´), 145.6 (C-7), 147.8 (C-2), 152.9 (C-6), 165.7 (COOH), 176.0 (C= O). Figure 3C shows the 13C RMN for IC; both CIP and βCD Ccarbonyl and Cketone peaks have a slight shift (1 and 2 ppm); the CH_2 from piperazine is also seen (2 ppm). The C1 from βCD overlaps with signals from CIP. The multiple resonances of the carbons of the CIP molecules converge to a single peak in the IC suggesting that the CIP units adopt a more symmetrical conformation in the complex than in bare CIP.

4.2 Fibers characterization

The fibrous components were analyzed by Raman spectroscopy (Figure 4). The major absorption peak for PLA fibers appeared at 3000 cm^{-1} and 2950 cm^{-1}; these are attributed to the CH_3 asymmetric and symmetric stretch bending vibration followed by 1750 cm^{-1} C=O symmetric stretching vibration and a 990 cm^{-1} Cester-Cα vibration. The principal CIP absorption bands are at 1613 cm^{-1} from C=O pyridine as well as 1580 and 1382 cm^{-1} from O-C-O asymmetric and symmetric, respectively. In PLA-CIP fibers, the principal bands of PLA and CIP are present indicating the incorporation of CIP into PLA fibers.

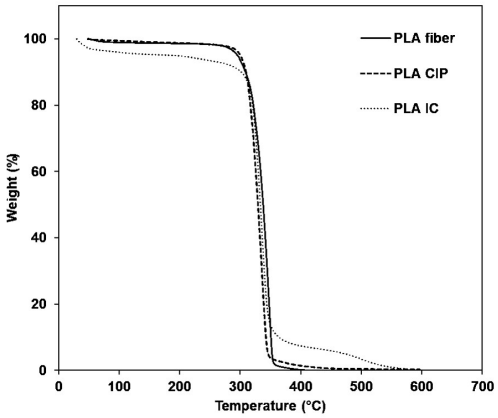

Fig. 5. Thermal characterization of PLA, PLA-CIP, and PLA-IC fibers.

The presence of cyclodextrin PLA-IC conceals the CIP signal; only PLA peaks are seen.

TGA data is shown in Figure 5. At 5% wt loss, both PLA and PLA-CIP fibers show PLA degradation-the CIP percentage in the PLA fibers is insufficient to change the degradation of the PLA fibers. In PLA/CIP/βCD-IC, the addition of the inclusion complex modifies the degradation behavior of PLA fibers starting with the dehydration of non-complexed cyclodextrin. All samples were degraded at 500 °C.

Figure 6 shows the SEM images and diameter size distribution of PLA fiber, PLA-CIP, and PLA-IC. The diameter was determined through ImageJ software using an average of 150 fibers. The fibers have a smooth surface, and they are heterogeneous diameters and orientations (Fig. 6a). When the fiber is loaded with drug, the morphology and diameter size are only similar to PLA (Fig. 6b) indicating that the addition of CIP to the feed solution does not affect the spinning process at low CIP concentrations. Fibers containing the IC have an average size of 300 to 400 nm; larger diameter sizes are also seen because of the presence of beads. The SEM images show the dependence of drug content versus fiber diameter-this impacts the timed release.

4.3 Loading efficiency (LE%)

The LE for the three samples fabricated on three different days (LE%) was determined by Equation 1. The CIP from PLA-CIP and PLA-IC was quantified by UV-Vis (Table 1). The LE% of samples that contain the IC was superior to that of fibers with only CIP confirming the better compatibility and solubility of

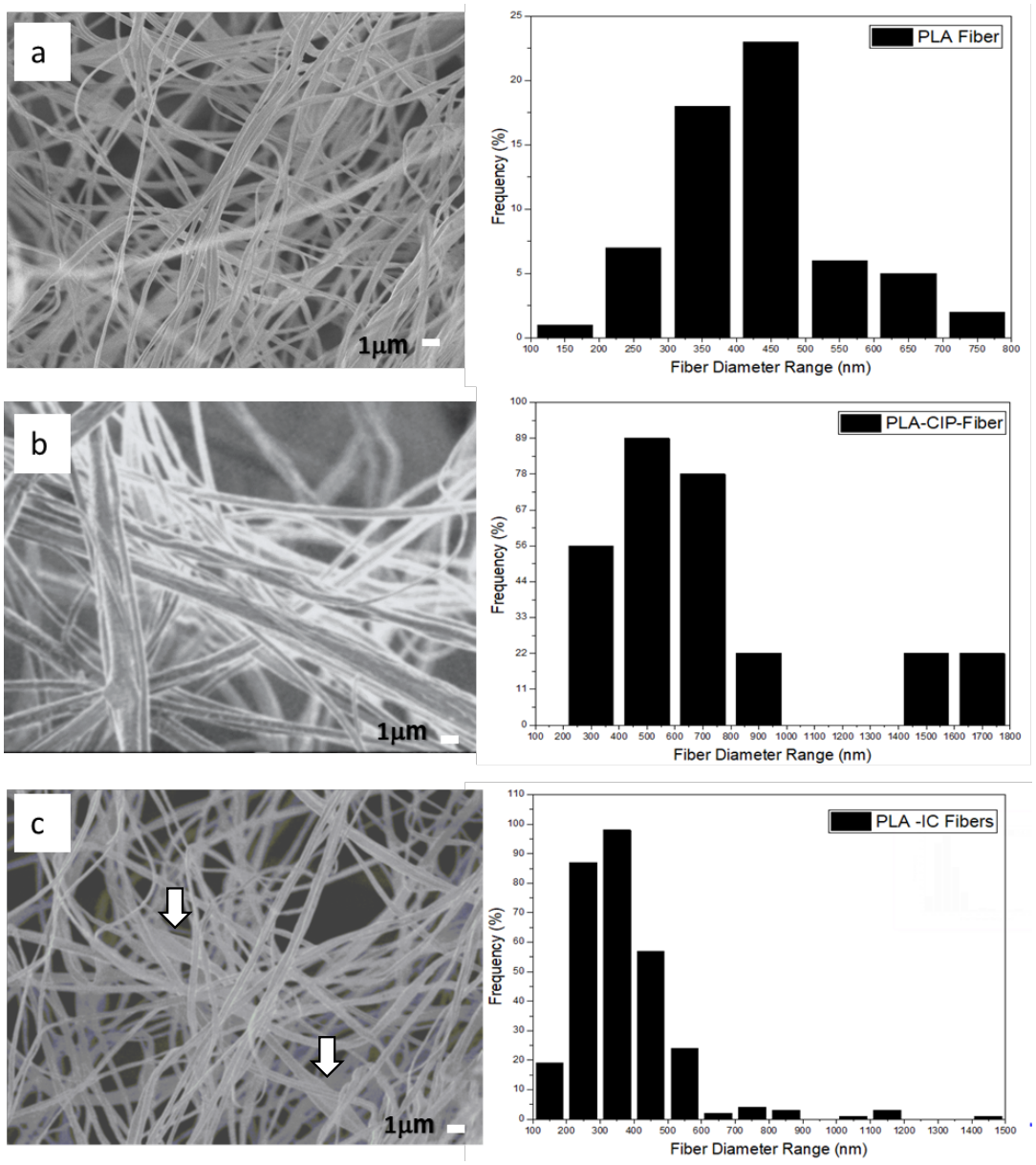

Fig. 6. SEM micrograph of fiber diameter distribution of a) PLA fiber, b) PLA-CIP fiber, and c) PLA-IC fiber obtained at CIP content 10 wt% with respect to the polymer content.

Table 1. Loading efficiency for three different samples by triplicate measurements of PLA- CIP fibers and PLA-IC 10 wt% of CIP.

	Sample	Loading Efficiency (%) n=3
PLA- CIP- fiber	1P-CIP10	36 ± 1.2
	2P-CIP10	44 ± 1.7
	3P-CIP10	32 ± 2.4
PLA-IC-fiber	1P-IC10	98 ± 0.3
	2P-IC10	96 ± 0.5
	3P-IC10	101 ± 1.6

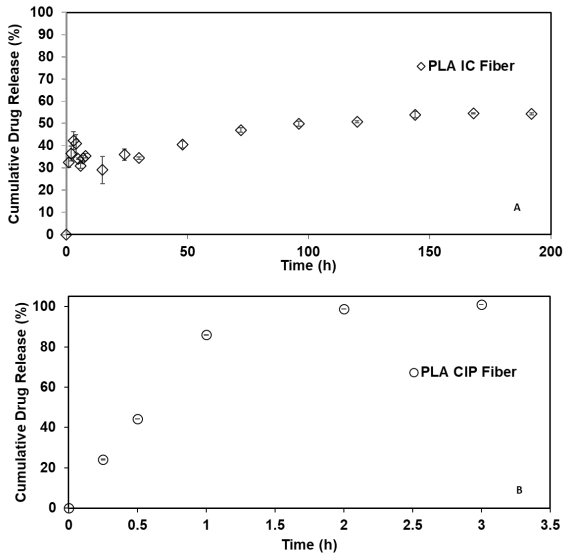

Fig. 7. Fitted curves of ciprofloxacin release of the O PLA-CIP and ◊ PLA-IC fibers.

IC in PLA solution during encapsulation. The milky CIP suspension in DCM: DMSO was not stable during electrospinning process; high amounts of drug were lost during electrospinning process by precipitation of CIP. The major IC solubility in PLA solution, improves the drug encapsulation in polymer fibers Table 1. Loading efficiency for three different samples by triplicate measurements of PLA- CIP fibers and PLA-IC 10 wt% of CIP.

4.4 In vitro release study

The release of CIP from the PLA-CIP fiber and PLA-IC fiber into PBS was measured at 37 °C by UV-Vis at 276 nm; the results are shown as cumulative drug release versus time (Fig. 7). The release of CIP from PLA-CIP was faster because the burst effect was reached during the first 120 min with 100% drug release. These effects could be because the CIP was not sufficiently dispersed in the initial suspension in addition to the incompatibility of the polymer, solvent, and drug. This would result in ciprofloxacin loading mainly on the fiber surface. The profiles of PLA-IC after a quick burst release were linear and slow, i.e., about 50% of the drug was released over 8 days showing a typical dual stage release profile-the initial relatively fast release was followed by a constant release, on the other hand, CIP in the IC was loaded on the fiber surface-there was an initial burst phase (first 3 h) and more controlled secondary phase (5-8 days) that were loaded in the fiber bulk. The burst effect of the IC could be because a little quantity of IC was encapsulated close to the surface. This might be crucial for many applications that are related to the prevention of bacteria proliferation because a higher release at the initial stage is important. This limits the proliferation of bacteria in the beginning, while sustained release inhibits the few bacteria that managed to proliferate (Kim, *et al*., 2004). The entry of solvent into the polymer that is in the vitreous state produces a considerable increase in the mobility, which implies a decrease in the glass transition temperature, Tg. The solvent-polymer compatibility can be expressed by the solubility parameter and the polymer-solvent interaction. If the solvent is poorly compatible with the polymer, the decrease is not sufficient for the polymer to reach its elastomeric state (Virginia, *et al*., 2004).

When the system reaches the thermodynamic equilibrium, the polymer will be in the vitreous state, and under these conditions, the release of the drug becomes very slow. In the case of the system PLA-Buffer solution as a release medium, the incompatibility is evident, when CIP or IC is releasing, the water buffer solution does not swell the polymer matrix. It means that CIP or IC release is no governed by solvent instead it is a diffusion process where the transport of the drug is due to the dissolution of the solute in the solvent by polymer interface and its subsequent diffusion to the outside, through the fibers segments, under the influence of a concentration gradient that follows Fick's First Law, nevertheless in the case of IC, the drug was loaded in the bulk of the fiber, increasing the polymer interface with the release medium slowing down the release of IC. In the case of only CIP and due to the poor solubilization before electrospinning, the release is faster because the drug is located, in its majority, in the border between PLA fiber and PBS buffer medium.

The maximum amount release of CIP from PLA-IC was 3 μg per day. As mentioned before, this situation is related to the existence of βCD in the matrix, the initial solubilization, and the IC formation (Szejtli, 1998). The presence of beads in the IC and the fiber size were not determining parameters that affected the release profile.

To determine the release kinetics and models, drug release data from PLA-CIP and PLA-IC were kinetically evaluated and fitted to the three different kinetic models including Korsmeyer-Peppas, zero-order, and first order. In addition, the presence of CD can lower the required dose of an active molecule by improving its solubility (Bibby, *et al*. 2000).

Table 2. Kinetic model parameters for dosage forms PL-CIP and PLA-IC fibers.

Kinetic Model	Parameter	PLA-CIP Fiber	PLA-IC Fiber
Korsmeyer-Peppas	R^2	0.936	0.740
	K_P	66.64	32.666
	n	0.434	0.083
First-Order	R^2	0.920	0.934
	K	-1.709	-0.002
Zero-Order	R^2	0.756	0.916
	K	26.21	34.113

The *in vitro* drug release data from PLA-CIP and PLA-IC were kinetically evaluated and fitted to the Korsmeyer-Peppas, zero-order, and first order models. These models are commonly used in the drug release kinetic studies because of their applicability and simplicity. Korsmeyer-Peppas model is generally used to examine the release of drugs from polymeric dosage forms, when the release mechanism is not well known or when more than one type of release phenomena could be involved and also the model includes some parameters that can explain the mechanisms release for porous pharmaceutical dosage forms as a nano and microfibers mats. Zero-order, and first order models best describe the process of drug release from pharmaceutical dosage forms and even polymeric matrices. The release kinetic mechanism is described by the following equations: Equation 2, Korsmeyer-Peppas; Equation 3, the zero-order model; and Equation 4, first-order model.

$$\frac{M_t}{M_\infty} = K_P t^n \tag{2}$$

$$\frac{M_t}{M_\infty} = K_0 t \tag{3}$$

$$\ln \frac{M_t}{M_\infty} = -K_1 t \tag{4}$$

Here, M_t/M_∞ is the fraction of drug released at any time t; K_P, K_o, and K_1 are release rate constants. The constant n for Korsmeyer-Peppas model is the diffusional exponent indicative of mechanism of drug release; n ≤ 0.45 indicates a classical Fickian diffusion-controlled (case I) drug release. Values of n between 0.45 and 0.89 indicate both phenomena (drug diffusion in the hydrated matrix and the polymer relaxation). This is commonly called anomalous transport. Values of n ≥ 0.89 indicates super case II (zero-order) (Tamaddon, *et al*., 2015; Korsmeyer, and Peppas, 1981; Korsmeyer, *et al*., 1983).

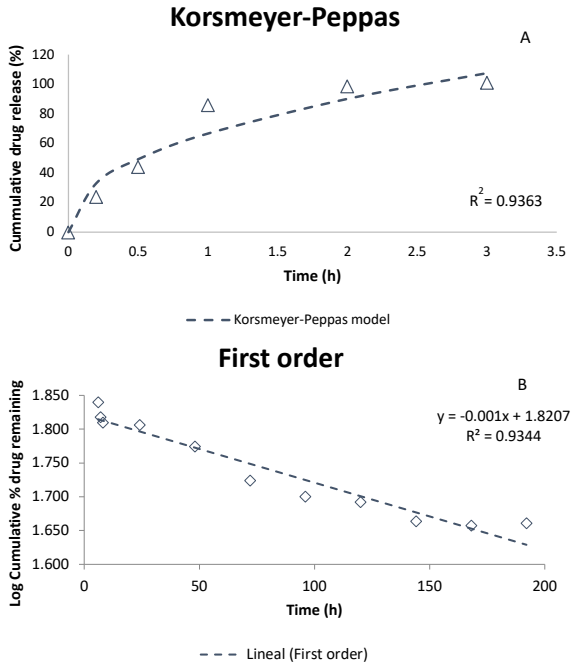

Fig. 8. Fitted curves of ciprofloxacin release of the (A) PLA-CIP and (B) PLA-IC fibers to Korsmeyer-Peppas and first-order mathematical models. The dotted line represents the fit curve.

Table 2 shows the adjustment parameters for each model. Micro and nanofiber mats were evaluated and compared in the release kinetic pattern to demonstrate the impact of the ciprofloxacin IC. Plots for the better adjusted models are shown in Figure 8.

The best model fit was based on correlation coefficient (R^2) values. While no single kinetic model that could explain the entire release profile, the best R^2 for CIP in PLA-CIP was showed with the Korsmeyer-Peppas model (R^2 =0.9363). The Korsmeyer-Peppas model describes: a) the release profile of polymeric pharmaceutical forms, b) ill-defined release mechanisms, and c) more than two types of release mechanisms. The value of exponential

factor "n" (0.43) indicates release of CIP from the PLA fiber matrix. This refers to a classical Fickian diffusion-controlled (case I) drug release.

The entire release profile was best described by first-order model for PLA-IC fiber ($R^2 \sim 0.9344$) (Table 2). The pharmaceutical formula that follows this profile monitors the amount of drug proportional to the amount remaining per unit time; thus, the amount of drug released decreases (Mulye, V. and Turco, 1995). In the release process (Fig. 8B), the first stage is the "burst" effect. This occurs due to a superficial desorption. As the release progresses, the slope approaches zero, which indicates that less ciprofloxacin is released according to a first-order model (Eq. 3).

The presence of cyclodextrin modifies the release profile mechanism when compared with only CIP and has a bigger influence on release time. The release of CIP as well as PLA-CIP from PLA- IC will be zero at any time. This can continue over time in PLA-IC until the drug is released by degradation of PLA. The release then will depend on the degradation rate of the PLA (Rueda, *et al*. 2016). Cyclodextrin encapsulates ciprofloxacin and delays its release leading to 50% of IC being released at 192 h versus 100% in 3 h without cyclodextrin.

In this case Order Zero model don't be adequate to evaluate the mechanism. The correlation coefficient was 0.75 and 0.91 to PLA-CIP and PLA-IC respectively that was lower than first order to PLA-IC and Korsmeyer-Peppas to PLA-CIP.

The K value is higher for PLA-CIP than that with PLA-IC due to an increase in the solvent volume embedded in the pores between fibers over 8 days of experiments. The presence of cyclodextrin in the PLA fibers increases the hydrophilicity of the system indicating that the process is governed by dissolution and that the IC is dispersed on the fiber bulk and surface.

Conclusions

In summary, we prepared CIP and IC composite PLA microfibers via electrospinning. The drug was stable during the spinning process as confirmed by UV-Vis absorption. The loading efficiency for PLA-IC was better than PLA-CIP because ciclodextryn improves the drug encapsulation and solubility. The incorporation of ciclodextryn can enhance drug release from polymeric systems because they increase the concentration of diffusible species within the matrix and facilitate drug release, but in this case CDs shown to be effective improving encapsulation of CIP onto micro and nanofibers, but has not the hydrophilic influence in release mechanism due to it was encapsulated onto the bulk of nanofibers plus the poor swelling of PLA in PBS medium. Nevertheless, CIP showed sustained and controlled release only when encapsulated in the CD. The PLA-CIP system was better adjusted to the Korsmeyer-Peppas model, and the PLA-IC was fitted to the first-order model because of the cyclodextrin improved the release of ciprofloxacin delaying the release rate. Based on this result PLA-IC fiber could be used as a sustained-release system.

Acknowledgements

We appreciate the Electron Microscopy Facility of UAM-I and Patricia Castillo Ocampo for SEM images. We acknowledge CONACYT CB16RF_287927 project and other support from CONACYT INFR18_RF293350.

Nomenclature

Ce	concentration of encapsulated active compound, mg mL^{-1}
Ct	total concentration of the active compound, mg mL^{-1}
K1	first order constant
Ko	order Zero constant
Kp	Korsmeyer-Peppas constant
LE%	loading efficiency, percentage
$M_t M_\infty^{-1}$	fraction of drug released at any time
T	time, min

References

Ahire, J.J., Neveling, D.P., Hattingh, M. and Dicks, L.M.T. (2015). Ciprofloxacin-Eluting Nanofibers Inhibits Biofilm Formation by Pseudomonas aeruginosa and a Methicillin-Resistant *Staphylococcus Aureus. PLoS ONE 10*, 1-13. DOI: 10.1371/journal.pone.0123648.

Auras, R., Harte, B., and Selke, S. (2004). An overview of polylactides as packaging materials. *Macromolecular Bioscience 4*, 835 - 864. doi.org/10.1002/mabi.200400043.

Aytac, Z., Sen, H.S., Durgun, E. and Uyar, T. (2015) Sulfisoxazole/cyclodextrin inclusion complex incorporated in electrospun hydroxypropyl cellulose nanofibers as drug delivery system. *Colloids and Surfaces B: Biointerfaces 128*, 331-338. DOI: 10.1016/j.colsurfb.2015.02.019.

Bibby, D.C., Davies, N.M. and Tucker, I.G. (2000) Mechanisms by which cyclodextrins modify drug release from polymeric drug delivery systems. *International Journal of Pharmaceutics 197*, 1 - 2. DOI: 10.1016/S0378-5173(00)00335-5.

Bottino, M.C., Arthur, R.A. Waeiss, R.A., Kamocki, K., Gregson, K. S. and Gregory, R.L. (2014). Biodegradable nanofibrous drug delivery systems: effects of metronidazole and ciprofloxacin on periodontopathogens and commensal oral bacteria. *Clinical Oral Investigations 18*, 2151-2158. DOI: 10.1007/s00784-014-1201-x.

Bukovec, I. T. P. and Quirds, M. (1997). Crystal structure of ciprofloxacin hexahydrate and its characterization. *International Journal of Pharmaceutics 152*, 59-65. DOI: 10.1016/S0378-5173(97)04913-2.

Buvári, Á., Barcza, L. and Kajtár, M. (1988). Complex formation of phenolphthalein and some related compounds with β-cyclodextrin. *Journal of Chemical Society Perkin Transactions 2*, 1687-9160. DOI: 10.1039/P29880001687.

Choia, Y., Nirmala, R., Lee, J. Y., Rahman, M., Hong, S.T. and Kima, H.Y. (2013). Antibacterial ciprofloxacin HCl incorporated polyurethane composite nanofibres via electrospinning for biomedical applications. *Ceramics International 39*, 4937 - 4944. DOI: 10.1016/j.ceramint.2012.11.088.

Greiner, A., and Wendorf, J. H. (2007). Electrospinning: a fascinating method for the preparation of ultrathin fibers. *Angewandte Chemie International 46*, 5670 -5703. DOI: 10.1002/anie.200604646.

Jannesari, M., Varshosaz, J., Morshed, M. and Zamani, M. (2011). Composite poly(vinyl alcohol)/poly(vinyl acetate) electrospun nanofibrous mats as a novel wound dressing matrix for controlled release of drugs. *International Journal of Nanomedicine 6*, 993 - 1003. DOI: 10.2147/IJN.S17595.

Jianbin, C., Liang, C., Hao, X., and Dongpin, M. (2002). Preparation and study on the solid inclusion complex of ciprofloxacin with beta-cyclodextrin. *Spectrochimica Acta Part A 58*, 2809-2815. DOI: 10.1016/S1386-1425(02)00078-1.

Kim, K., Luu, Y.K., Chang, C., Fang, D., Hsiao, B.S., Chu, B. and Hadjiargyrou, M. (2004). Incorporation and controlled release of a hydrophilic antibiotic using poly(lactide-co-glycolide)-based electrospun nanofibrous scaffolds. *Journal of Control Release 98*, 47 - 56. DOI: 10.1016/j.jconrel.2004.04.009.

Korsmeyer, R. W., Gurn, R., Doelker, E., Buri, P. and Peppas, N.A. (1983). Mechanism of solute release from porous hydrophilic polymers. International Journal of Pharmaceutics, 3(15), 25-35. DOI: 10.1016/0378-5173(83)90064-9.

Korsmeyer, R.W. and Peppas, N. A. (1981). Macromolecular and modeling aspects of swelling-controlled systems. In: *Controlled Release Delivery Systems*. Roseman, T.J., Mansdorf, S.Z., eds. New York: Marcel Dekker, 77-90.

Ledezma-Oblea, J.G., Morales-Sanchez, Gaytan-Martínez, E. M., Figueroa-Cardenas, J.D., Gaona-Sanchez, V.A. (2015). Corn starch nanofilaments obtained by electrospinning. *Revista Mexicana de Ingeniería Química 14*, 597-502. DOI:

Mulye, V. and Turco, S.J.A. (1995). A simple model based on first-order kinetics to explain the release of highly water-soluble drugs from porous di-calcium phosphate dihydrate matrices. *Drug Development and Industrial Pharmacy 21*, 943-953. https://doi.org/10.3109/03639049509026658.

Rajendiran, N., Mohandoss, T., and Thulasidhasanm, J. (2016). Encapsulation of ciprofloxacin, sparfloxacin, and ofloxacin drugs with α- and β-cyclodextrins: spectral and molecular modelling studies. *Physics and Chemistry of Liquids 54*, 193 - 212. DOI:10.1080/00319104.2015.1074046.

Rueda, C., Vallejo, I., Corea, M., Palacios, E. G., Chairez, I. (2015). Degradation study of poly(lactic-l(+)-co-glycolic acid) in chloroform. *Revista Mexicana de Ingeniería Química 14*, 813-827. http://rmiq.org/iqfvp/Pdfs/Vol.%2014,%20No.%203/Poli1/Poli1.html.

Salgado-Delgado, A.M., Vargas-Galarza Z., Salgado-Delgado, R., Garcia-Hernandez, E., Hernandez-Díaz, W.N., Rubio-Rosas, E., Salgado-Rodriguez, R. (2016). Morphological and thermal characterization of a high porous composite of biomaterial phema-chitosan-ceramic (hydroxyapatite). *Revista Mexicana de Ingeniería Química 15*, 625-632. http://www.rmiq.org/iqfvp/Pdfs/Vol.%2015,%20No.%202/Mat1/RMIQTemplate.pdf.

Shawki, M.; Hereba, A. and Ghazal, A. (2010). Formation and characterization of antimicrobial dextran nanofibers. *Romanian Journal of Biophysics 20*, 335 - 346. DOI: 10.1016/j.carbpol.2004.05.013.

Szejtli J. (1994). Cyclodextrins in Pharmacy Topics in *Inclusion Science* Edi. by Karl-Heinz Frömming Springer Netherlands Publisher, Amsterdam, 1-18. DOI: 10.1007/978-94-015-8277-3.

Szejtli, J. (1988). Cyclodextrin inclusion complexes. In: *Cyclodextrin Technology*. Topics in Inclusion Science, Springer, Dordrecht, 79-185. DOI: 10.1007/978-94-015-7797-7.

Tamaddon, L., Mostafavi, S.A., Karkhane, R., Riazi-Esfahani, M., Dorkoosh, F.A. and Rafiee-Tehrani, M. (2015). Design and development of intraocular polymeric implant systems for long-term controlled-release of clindamycin phosphate for toxoplasmic retinochoroiditis. *Advanced Biomedical Research 4*, 32-43. DOI: 10.4103/2277-9175.150426.

Toncheva, A., Paneva, D., Maximova, V., Manolova, N. and Rashkov, I. (2012) Antibacterial fluoroquinolone antibiotic-containing fibrous materials from poly(L-lactide-co-D,L-lactide) prepared by electrospinning. *European Journal of Pharmaceutical Science 47*, 642 -651. DOI: 10.1016/j.ejps.2012.08.006.

Virginia Sáez, Estibaliz Hernáez and Lucio Sanz Angulo. (2004). Mecanismos de liberación de fármacos desde materiales polímeros. *Revista Iberoamericana de Polímeros 5*, 55-70.

Wendorff J.H., Agarwal S. and Greiner A. (2012). *Electrospinning Materials Processing and Applications*, ed by Smith G. John Wiley & Sons Publishing, Weinheim, p 254.